Tuning open-circuit voltage in organic solar cells by magnesium modified Alq_3

Chi-Ta Chou,[1] Chien-Hung Lin,[2] Meng-Hsiu Wu,[3] Tzu-Wei Cheng,[4] Jiun-Haw Lee,[2] Chin-Hsin J. Liu,[1] Yian Tai,[1] Surojit Chattopadhyay,[5,a)] Juen-Kai Wang,[6] Kuei-Hsien Chen,[3,6] and Li-Chyong Chen[6,a)]
[1]*Department of Chemical Engineering, National Taiwan University of Science and Technology, Taipei 106, Taiwan*
[2]*Graduate Institute of Photonics and Optoelectronics and Department of Electrical Engineering, National Taiwan University, Taipei 106, Taiwan*
[3]*Institute of Atomic and Molecular Sciences, Academia Sinica, Taipei 106, Taiwan*
[4]*Institute of Organic and Polymeric Materials, National Taipei University of Technology, Taipei 106, Taiwan*
[5]*Institute of Biophotonics, National Yang Ming University, Taipei 112, Taiwan*
[6]*Center for Condensed Matter Science, National Taiwan University, Taipei 106, Taiwan*

(Received 6 May 2011; accepted 13 September 2011; published online 20 October 2011)

The low molecular weight tris-(8-hydroxyquinoline) aluminum (Alq_3) has been incorporated with magnesium (Mg) that altered the nature of its opto-electronic characteristics. The lowering of the highest occupied molecular orbital (HOMO) and lowest unoccupied molecular orbital (LUMO) in Mg:Alq_3, compared to pure Alq_3, creates a stronger field (exceeding the exciton binding energy) at the donor-acceptor junction to dissociate the photo-generated exciton and also provides a low barrier for electron transport across the device. In an electron-only device (described in the text), a current enhancement in excess of 10^3, with respect to pure Alq_3, could be observed at 10 V applied bias. Optimized Mg:Alq_3 layer, when introduced in the photovoltaic device, improves the power conversion efficiencies significantly to 0.15% compared to the pure Alq_3 device. The improvement in the photovoltaic performance has been attributed to the superior exciton dissociation and carrier transport. © *2011 American Institute of Physics*. [doi:10.1063/1.3653259]

I. INTRODUCTION

Exciton dissociation is one of the keys to the performance of organic photovoltaic devices (OPVDs) and is known to occur at the organic semiconductor/metal interface or between the electron and hole transport layers known as acceptors (A) and donors (D), respectively.[1–8] Organic materials with sufficient separation, in energy, of the lowest unoccupied molecular orbital (LUMO) offsets between donor and acceptor are good junctions for exciton dissociation.[1–3] It was found that not the open circuit voltage (V_{oc}) but the short circuit current density (J_{sc}) is the limiting factor for obtaining high efficiency with the current state of technology. Also an empirical threshold of 2.0 eV was found between the LUMOs of the donor and the acceptor, necessary for the exciton dissociation.[1] The observed lowering of the driving force, or internal electric field, for exciton dissociation effect at the donor/acceptor interface may be a limitation to further enhancements in photocurrent generation.[2] In addition to the separation of the highest occupied molecular orbital ($HOMO_D$) and $LUMO_A$, it was favorable for determining V_{oc}.[4–8] The quantity, $HOMO_D$—$LUMO_A$, controls the performance of the OPVDs, through changes in the open-circuit voltage (V_{oc}).[9–13]

Tris-8-hydroxyquinolin aluminum (Alq_3) having a high internal quantum yield and a stable electrical conductivity is a state-of-the-art green emission and an electron transporting material in organic light-emitting diodes (OLEDs).[14,15] Several alkaline metals, such as Li, Ca, and Mg (Ref. 16) have been added to the acceptor material, Alq_3, in the cathodes of OLEDs to promote electron injection and to increase electrical conductivity.[17–23] The interaction of the reactive metals might be occurring within the quinoline ligand of Alq_3. In Mg:Alq_3 case, the N 1*s* core shifts to a lower binding energy indicating an Mg-induced charge-transfer component.[24–26] X-ray photoelectron spectroscopy (XPS) and ultraviolet photoemission spectroscopy (UPS) revealed that the Mg clusters can significantly affect the adjacent quinoline ligand, and the charge in oxygen on the phenoxide side is pulled towards the nitrogen on the pyridyl side of the quinoline ligand.[27] In those studies, the incorporation of Al, Ca, or Mg in Alq_3, resulted in the formation of a gap state that modified the Alq_3 HOMO and lowered the barrier for electron injection in organic devices.

The present work takes up the challenge of designing an inexpensive and stable organometallic compound, with a high HOMO, using Mg modification of Alq_3 that can be promising in photovoltaic (PV) applications. We present a detailed opto-electronic description of the Mg:Alq_3 complex, prepared by co-evaporation, which is different from the reported bi-layer structure in OLEDs. The shifts of the electronic energy levels in Mg:Alq_3, as a function of the Mg incorporation, were analyzed using UPS and optical absorption measurement,[28] and its effect on the open circuit voltage of the ZnPc/Mg:Alq_3 photovoltaic device was carried out.

a)Author to whom correspondence should be addressed. Electronic addresses: chenlc@ntu.edu.tw and sur@ym.edu.tw.

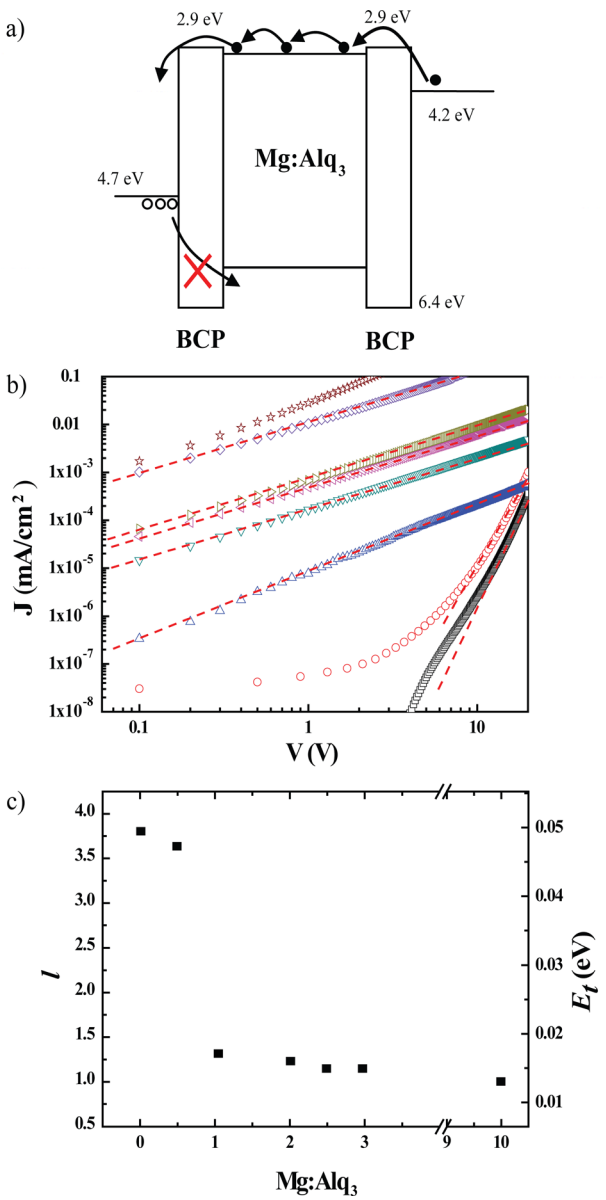

FIG. 1. (Color online) (a) The energy diagram of the ITO/BCP (20 nm)/Mg:Alq_3 (100 nm)/BCP (20 nm)/LiF (1.2 nm)/Al (100 nm) device with different Mg:Alq_3 ratio. The BCP is an electron injection layer and a hole blocker. (b) I-V characteristics of the ITO/BCP/Mg:Alq_3/BCP/LiF/Al electron-only devices made with different Mg: Alq_3 ratio and the double-logarithmic representation with fits to power lows $J \propto V^{l+1}$. (☆)Mg; (◇)Mg:Alq_3 = 10:1, $l+1=2.0$; (▷)3:1, $l+1=2.1$; (◁)2.5:1, $l+1=2.1$; (▽)2:1, $l+1=2.2$; (△)1:1, $l+1=2.3$; (○)0.5:1, $l+1=4.6$; (□)Alq_3, $l+1=4.8$. (c) The distribution of l parameter with Mg:Alq_3 ratio.

II. EXPERIMENTAL

We attempted different mixing ratio of Mg and Alq_3 in depositing a film by a simple co-evaporation method. Thin films with co-deposition ratio Mg:Alq_3 of 0:1, 0.5:1, 1:1, 2:1, 2.5:1, and 3:1 were defined by individual quartz-crystal thickness monitors. The deposition rate of Alq_3 was fixed at 0.5 Å/s using a constant 300 °C temperature of the quartz cell. The Mg deposition rate was varied from 0 to 1.5 Å/s, using different temperatures to achieve different mixing ratios. The actual PV devices with the organometallic complex as *n*-type layer had the following structure: glass/ITO/PEDOT:PSS/zinc-phthalocyanine (ZnPc) (50 nm)/Mg:Alq_3 (90 nm)/Al (150 nm). The ITO-coated glass was cleaned by the standard procedure (cleaning and sonication in detergent solution followed by sonication in acetone and isopropyl alcohol). A buffer layer of poly(ethylenedioxythiophene) doped with poly(styrenesulfonate) (PEDOT:PSS), with a thickness of about 30 nm, was obtained by coating an aqueous solution onto the ITO-coated glass substrates. Subsequent layers were fabricated via vacuum deposition with a base pressure of around 8×10^{-6} Torr. The ZnPc were adopted as electron donor and the Mg:Alq_3 acted as the electron acceptor in the device, respectively. The active area of the solar cell was 0.04 cm^2. The current-voltage (I-V) characteristics of the solar cells were measured in the dark and illuminated conditions using AM1.5 G solar illumination at 100 $mWcm^{-2}$ (Thermal Oriel 500 W solar simulator). The valence states were recorded using the He I (21.2 eV) and He II (40.8 eV) radiation lines from a gas discharge lamp in the UPS studies. The samples for UPS were prepared on Au substrates and the first layer of Alq_3 (15 Å) was used as a reference.[28]

III. RESULTS AND DISCUSSION

The electron-transport properties of organic materials, such as Alq_3, have been investigated intensively, by their *J-V* characteristics, in the past due to their application in OLEDs.[29] To fabricate the electron-only devices, Alq3 and Al were evaporated as the thin-film layer and top electrode, respectively. We have utilised a structure consisting of ITO/BCP (20 nm)/Mg:Alq_3 (100 nm)/BCP (20 nm)/LiF (1.2 nm)/Al (100 nm) with different Mg:Alq_3 ratio. The schematic energy level diagram of the device is shown in Fig. 1(a). The BCP was used as an electron injection layer and a hole blocker.

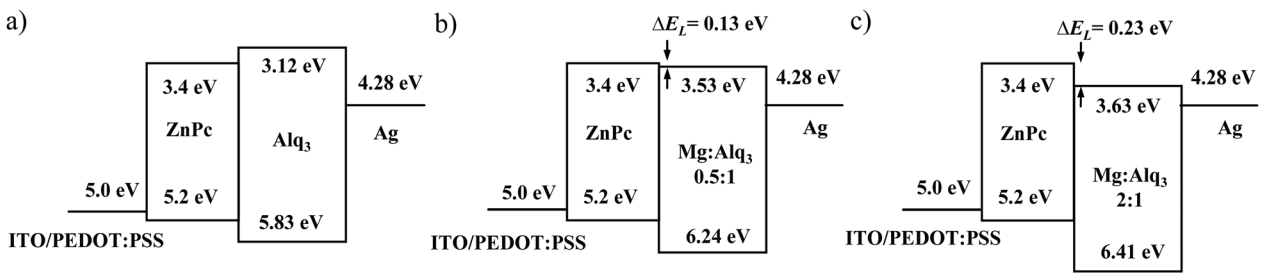

FIG. 2. Band diagram of ITO/ZnPc (50 nm)/Mg:Alq_3 (90 nm)/Ag (100 nm) photovoltaic devices with (a) pure Alq_3 (0:1), (b) 0.5:1, and (c) 2:1 of Mg:Alq_3.

Fig. 1(b) shows the experimental current density (J) of Mg:Alq_3 layers that were measured in electron-only device for different Mg:Alq_3 ratios. The devices were built on a BCP injection layer to avoid double-carrier injection. At lower bias, a remarkable enhancement in J could be observed with increasing Mg incorporation in the organic thin film. Even at 10 V, an enhancement of $\sim 10^3$ resulted in the J values for Mg:Alq_3 = 2.5:1 film with respect to the pure Alq_3. For the electron-only device, the trap-charge limited current (TCLC)[29] is given by,

$$J_{TCLC} = N_C \mu q \left(\frac{\varepsilon\varepsilon_0 l}{N_t q(l+1)}\right)^l \left(\frac{2l+1}{l+1}\right)^{l+1} \frac{V^{l+1}}{d^{2l+1}}, \quad (1)$$

where N_c is the density of states in the conduction band, N_t is the total trap density, μ is the carrier mobility, ε_0 is the free space permittivity, ϵ is the relative permittivity of the material, and d is the thickness of the active layer. The parameter $l = E_t/k_BT$, where E_t is the trap depth and k_BT is the thermal energy. A double-logarithmic plot yields a power law behaviour of the current density $J \propto V^{l+1}$ with different exponents $(l+1)$. A sharp decrease of l, and hence E_t, was observed with Mg introduction (Fig. 4(c)). The trap depth E_t decreases from 49 to 15 meV, with increasing Mg incorporation from 0 to 2:1 wt. % (Fig. 1(c)).

The Mg incorporation in Alq_3 thin films are shown to reduce the trap depth to enhance the carrier hopping motion. The J-V behaviour evolves from TCLC (for the devices with pure Alq_3) to space charge limited current (SCLC) regime in Mg:Alq_3. The electron-only devices exhibits enhanced electron-conducting property of the Mg modified Alq_3 thin films and its potential advantage in PV cells.

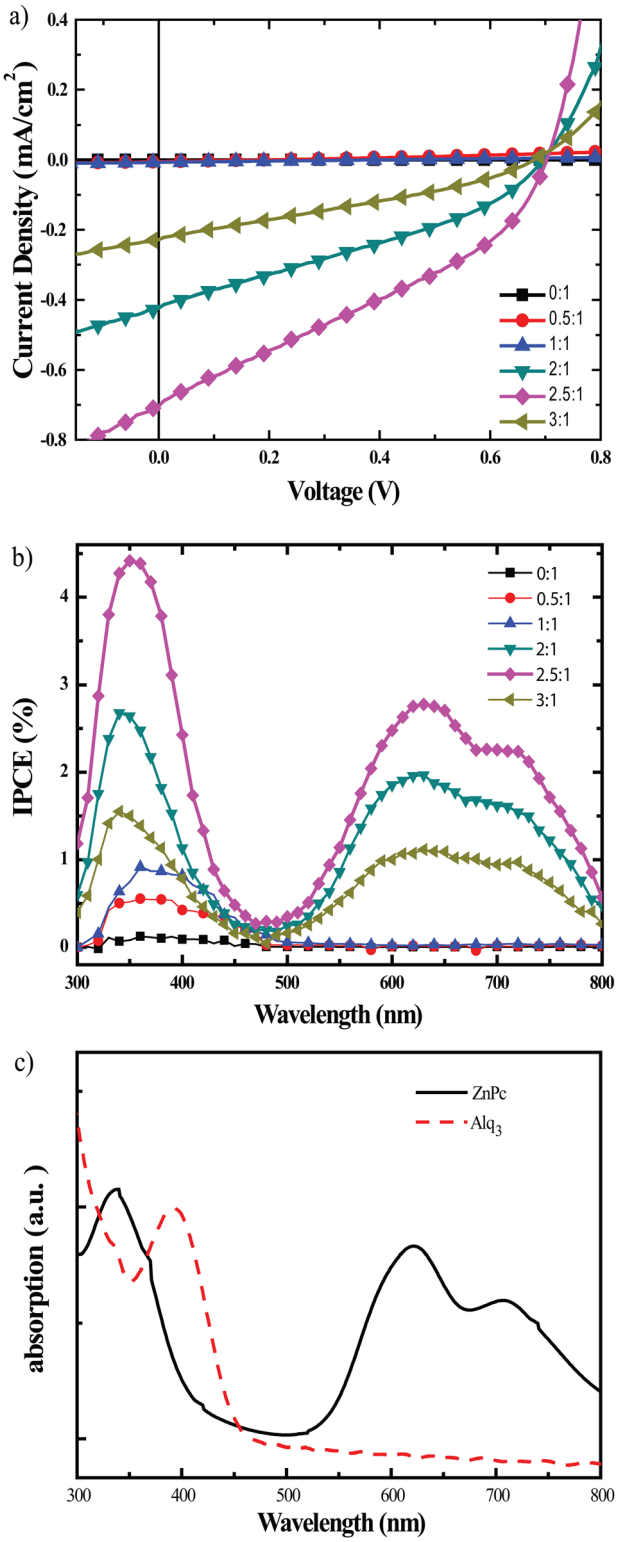

FIG. 3. (Color online) (a) The I-V curves, measured with AM1.5 G 100 mWcm^{-2} solar illumination, for devices using different mixing ratios of Mg:Alq_3. (b) The incident IPCE of the device, under short circuit conditions, for devices using different mixing ratios of Mg:Alq_3 thin films. (c) The absorption spectrum of ZnPc and pure Alq_3.

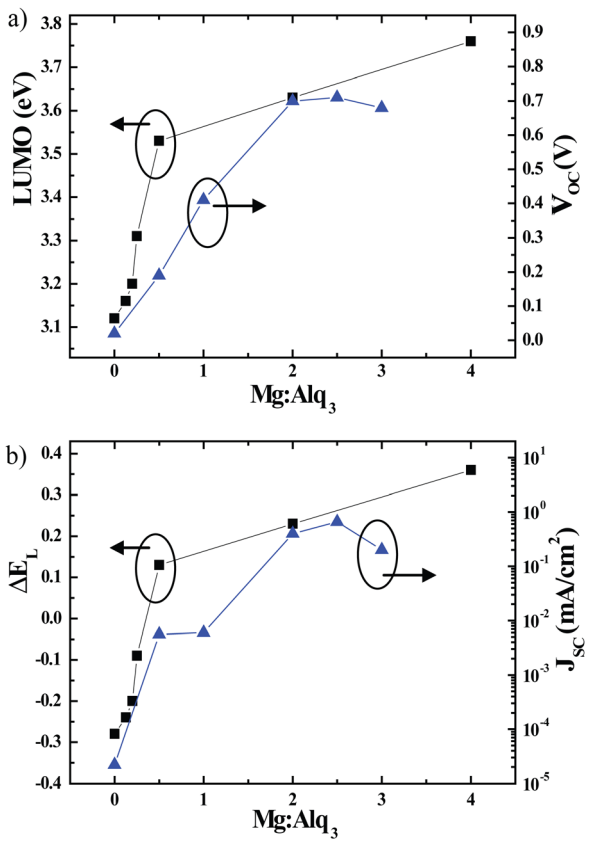

FIG. 4. (Color online) (a) The distribution of LUMO and V_{oc} and (b) the offset of the LUMO (ΔE_L) and J_{sc} as a function of Mg:Alq_3 mixing ratios.

The PV devices are now fabricated with zinc phthalocyanine (ZnPc) and Alq_3 junctions with ITO/PEDOT:PSS and silver (Ag) electrodes. Representative schematics of the energy diagram of the PV device with (and without) Mg is shown in Fig. 2. The shifts of electronic energy levels (HOMO, LUMO) in Mg:Alq_3, as a function of the Mg incorporation, were analyzed using UPS and optical absorption measurements,[28] while the HOMO and LUMO of pure Alq_3 was taken as -5.83 and -3.12 eV, respectively. The shift of the LUMO in Mg:Alq_3 towards the Ag Fermi level indicates a lowered barrier for electron injection in the device. Fig. 3(a) shows the *J-V* characteristic of the OPVDs fabricated with the Mg:Alq_3 as an electron transport layer under 100 mW/cm^2 AM1.5 G illumination. The device performance for pure Alq_3 is extremely poor with no detectable power conversion efficiency (η). By incorporating Mg, the *J-V* characteristic of the OPVDs can be significantly improved, with η value achieving 0.15%, optimized short-circuit current densities (J_{sc}) of 0.66 mA/cm^2, open-circuit voltage (V_{oc}) of 0.70 V, and a fill factor (*FF*) of 33.1%, for the device with Mg:Alq_3 (2.5:1) *n*-type layer (Table I). The *Rs* of the OPV devices are in accordance with the E_t result of the electron-only devices shown in Table I. The J_{sc} and *FF* are rather low for the OPV device. This may due to the low absorption in the visible region of Alq_3 and the high series resistance, suggesting that the thickness optimization of the active layer is necessary for further improvement.

The incident photon-to-current collection efficiency (IPCE) for devices with different Mg incorporation layers has been compared in Fig. 3(b). The best IPCE resulted from the device with Mg:Alq_3 (2.5:1) *n*-type layer. An excellent p-n junction with $HOMO_D$-$LUMO_A = 1.57$ eV for Mg-Alq_3 (2:1) layer is responsible for the gain in the J_{SC}. The best V_{oc} of 0.70 V is very close to the theoretical value[7,8] of 0.72 V calculated from

$$V_{oc} \leq (|LUMO_A - HOMO_D| - \Delta E)/q, \tag{2}$$

where $HOMO_D$ (~ 5.2 eV) is the HOMO of donor layer, $LUMO_A$ (~ 3.63 eV) is the LUMO of acceptor layer, ΔE (~ 0.85 eV) is sum of the difference between cathode Fermi level and acceptor LUMO ($4.28 - 3.63 = 0.65$ eV) and the anode Fermi level and donor HOMO ($5.2 - 5.0 = 0.2$ eV), and q is the elementary charge. Compared to the absorption spectra in Fig. 3(c), the IPCE spectrum, however, is dominated by the optical absorption spectrum of ZnPc. With excessive Mg in the *n*-type layer, the device performance was poor which may be due to severe clustering or agglomeration of the metal. Interestingly, with lower Mg incorporation ratio (1:1) also the device did not perform well indicating a narrow and critical window for Mg fraction in the modified organometallic layer. The distribution of the LUMO due to Mg incorporation clearly reflects in the variation of the V_{OC} as shown in Fig. 4(a) and Table II.

TABLE I. Parameters for the organic photovoltaic cells measured from the I-V result at room temperature for devices using different Mg:Alq_3 films. E_t is from the electron-only device measurement.

Mg:Alq_3	V_{oc} (V)	J_{sc} (mA/cm^2)	*FF* (%)	η (%)	*Rs* (kΩ/□)	E_t
0:1	0.02	2.2×10^{-5}	27	—	2.6×10^4	0.49
0.5:1	0.19	5.6×10^{-3}	24	2.6×10^{-4}	50	0.47
1:1	0.41	6×10^{-3}	24.3	5.9×10^{-4}	16	0.17
2:1	0.70	0.40	33.1	0.09	0.07	0.16
2.5:1	0.70	0.66	33.1	0.15	0.02	0.14
3:1	0.68	0.20	29	0.04	0.12	0.14

TABLE II. The electronic energy parameters (in unit of eV) for the doped Alq_3 samples.

Mg: Alq_3	HOMO	LUMO	ΔE_L
0:1	−5.83	−3.12	−0.28
1:8	−5.94	−3.23	−0.17
1:4	−6.12	−3.41	0.01
0.5:1	−6.24	−3.53	0.13
2:1	−6.41	−3.63	0.23
4:1	−6.54	−3.76	0.36

To assist in an efficient charge separation and free-carrier generation across the donor-acceptor interface, a certain offset of the LUMO and HOMO, i.e., ΔE_L (Fig. 2), is required.[30] This offset is often required to be higher than the exciton binding energy, E_B, in organic materials, but just sufficient to dissociate the exciton.[31] The exciton binding energy, E_B of ZnPc is measured to be 0.1 eV.[32] Hence, the condition for a favourable exciton dissociation would be

$$\Delta E_L > E_B. \tag{3}$$

The Mg:Alq_3 can provide a ΔE_L of 0.23 eV to overcome the ZnPc E_B of 0.1 eV for a Mg incorporation ratio exceeding 1:1. The LUMO level is ~ 3.63 eV, which corresponds to a $LUMO_A$-$LUMO_D$ offset of 0.23 eV, to ensure efficient electron transfer from the ZnPc to Mg:Alq_3. This expectation again is found to be true experimentally from the enhancement of the short-circuit current (Fig. 4(b)). Generally, this technique of metal modification of raw organic layers, such as Alq_3, offers a powerful pathway to tune the HOMO and LUMO levels, and to enhance charge separation and electron transport as a whole. Although the device parameters, such as efficiency, do not speak highly of the new device, but the percentage of improvement is impressive which can be attributed to this new Mg modification of the Alq_3.

IV. CONCLUSIONS

Tuning energy levels of molecular orbitals (HOMO, LUMO) in Alq_3 has been made possible by magnesium incorporation. Optimized Mg incorporation, ~2.5:1 wt. %, results in better electron transport properties compared to the pure Alq_3. In a standard organic photovoltaic device structure, such a Mg modified layer assist in achieving a near theoretical open circuit voltage of 0.72 V and a power conversion efficiency of 0.15% due to ideal band tuning. This technique of band alignment in organic molecules by metal incorporation, in general, may yield even better photovoltaic devices in the future.

[1]B. Minnaert and M. Burgelman, EPJ Appl. Phys. **38**, 111 (2007).
[2]M. Brumbach, D. Placencia, and N. R. Armstrong, J. Phys. Chem. C **112**, 3142 (2008).
[3]N. R. Armstrong, W. Wang, D. M. Alloway, D. Placencia, E. Ratcliff, and M. Brumbach, Macromol. Rapod Commun. **30**, 717 (2009).
[4]G. Dennler, M. C. Scharber, and C. J. Brabec, Adv. Mater. **21**, 1323 (2009).
[5]D. C. Olson, S. E. Shaheen, M. S. White, W. J. Mitchell, M. F. A. M. Van Hest, R. T. Collins, and D. S. Ginley, Adv. Funct. Mater. **17**, 264 (2007).
[6]L. J. A. Koster, V. D. Mihailetchi, and P. W. M. Blom, Appl. Phys. Lett. **88**, 093511 (2006).
[7]A. Liu, S. Zhao, S.-B. Rim, J. Wu, M. Könemann, P. Erk, and P. Peumans, Adv. Mater. **20**, 1065 (2008).
[8]D. Cheyns, J. Poortmans, P. Heremans, C. Deibel, S. Verlaak, B. P. Rand, and J. Genoe, Phys. Rev. B **77**, 165332 (2008).
[9]D. Veldman, S. C. J. Meskers, and R. A. J. Janssen, Adv. Funct. Mater. **19**, 1939 (2009).
[10]T. W. Ng, M. F. Lo, Y. C. Zhou, Z. T. Liu, C. S. Lee, O. Kwon, and S. T. Lee, Appl. Phys. Lett. **94**, 193304 (2009).
[11]C. J. Brabec, A. Cravino, D. Meissner, N. S. Sariciftci, T. Fromherz, M. T. Rispens, L. Sanchez, and J. C. Hummelen, Adv. Funct. Mater. **11**, 374 (2001).
[12]K. Vandewal, A. Gadisa, W. D. Oosterbaan, S. Bertho, F. Banishoeib, I. V. Severen, L. Lutsen, T. J. Cleij, D. Vanderzande, and J. V. Manca, Adv. Func. Mater. **18**, 2064 (2008).
[13]M. C. Scharber, D. Mühlbacher, M. Koppe, P. Denk, C. Waldauf, A. J. Heeger, and C. J. Brabec, Adv. Mater. **18**, 789 (2006).
[14]M. Segal, M. Singh, K. Rivoire, S. Difley, T. Van Voorhis, M. A. Baldo, Nature Mater. **6**, 374 (2007).
[15]C.-H. Hsiao, C.-F. Lin, and J.-H. Lee, J. Appl. Phys. **102**, 094508 (2007).
[16]A. Curioni and W. Andreoni, J. Am. Chem. Soc. **121**, 8216 (1999).
[17]H. Kaji, Y. Kusaka, G. Onoyama, and F. Horii, J. Am. Chem. Soc. **128**, 4292 (2006).
[18]J. Kido and T. Matsumoto, Appl. Phys. Lett. **73**, 2866 (1998).
[19]A. Rajagopal and A. Kahn, J. Appl. Phys. **84**, 355 (1998).
[20]M. A. Baldo and S. R. Forrest, Phys. Rev. B **64**, 085201 (2001).
[21]B. N. Limketkai and M. A. Baldo, Phys. Rev. B **71**, 085207 (2005).
[22]V. I. Arkhipov, P. Heremans, E. V. Emelianova, and H. Bässler, Phys. Rev. B **71**, 045214 (2005).
[23]M. G. Mason, C. W. Tang, L.-S. Hung, P. Raychaudhuri, J. Madathil, D. J. Giesen, L. Yan, Q. T. Le, Y. Gao, S.-T. Lee, L. S. Liao, L. F. Cheng, W. R. Salaneck, D. A. dos Santos, and J. L. Brédas, J. Appl. Phys. **89**, 2756 (2001).
[24]C. Shen, I. G. Hill, A. Kahn, and J. Schwartz, J. Am. Chem. Soc. **122**, 5391 (2000).
[25]C. Shen, A. Kahn, and J. Schwartz, J. Appl. Phys. **89**, 449 (2001).
[26]R. Q. Zhang, X. Y. Hou, and S. T. Lee, Appl. Phys. Lett. **74**, 1612 (1999).
[27]T.-W. Pi, C.-P. Ouyang, T. C. Yu, J. F. Wen, and H. L. Hsu, Phys. Rev. B **70**, 235346 (2004).
[28]C. H. Lin, C. T. Chou, Y. H. Chen, M. H. Wu, J. H. Lee, C. I. Wu, S. Chattopadhyay, C. H. J. Liu, K. J. Song, Y. Tai, J. K. Wang, K. H. Chen, and L. C. Chen, J. Appl. Phys. **109**, 083541 (2011).
[29]W. Brütting, S. Berleb, and A. G. Mückl, Org. Electron. **2**, 1 (2001).
[30]J.-L. Bredas, D. Beljonne, V. Coropceanu, and J. Cornil, Chem. Rev. **104**, 4971 (2004).
[31]V. D. Mihailetchi, L. J. A. Koster, J. C. Hummelen, and P. W. M. Blom, Phys. Rev. Lett. **93**, 216601 (2004).
[32]B. P. Rand, J. Genoe, P. Heremans, and J. Poortmans, Prog. Photovoltaics **15**, 659 (2007).